Superselective targeting using multivalent polymers

Galina V. Dubacheva[†]*, Tine Curk[§], Bortolo M. Mognetti[§‡], Rachel Auzély-Velty[⊥], Daan Frenkel[§], Ralf P. Richter[†‖▽◊]*

[†]Biosurfaces Unit, CIC biomaGUNE, Paseo Miramon 182, 20009 Donostia - San Sebastian, Spain; [§]Department of Chemistry, University of Cambridge, Cambridge CB2 1EW, United Kingdom; [‡]Center for Nonlinear Phenomena and Complex Systems, Université Libre de Bruxelles, Code Postal 231, Campus Plaine, B-1050 Brussels, Belgium; [⊥]Centre de Recherches sur les Macromolécules Végétales, CNRS, BP 53, 38041 Grenoble Cedex 9, France; Département de Chimie Moléculaire, Université Joseph Fourier, BP 53, 38041 Grenoble Cedex 9, France; [▽]Max-Planck-Institute for Intelligent Systems, Heisenbergstrasse 3, 70569 Stuttgart, Germany; [◊]Department of Biochemistry and Molecular Biology, University of the Basque Country, Barrio Sarriena s/n, 48940 Leioa, Spain.

Supporting information

1. Materials

Ethynylferrocene, β-cyclodextrin (β-CD), 6-monodeoxy-6-monoamino-β-cyclodextrin hydrochloride (β-CD-NH_3^+ Cl^-), 3-mercaptopropionic acid (MPA), *N*,*N*-diisopropylethylamine (DIEA), hydroxybenzotriazole (HOBt), *N,N′*-diisopropylcarbodiimide (DIC), 4-pentenoic anhydride, (tris[(1-benzyl-1H-1,2,3-triazol-4-yl)-methyl]amine (TBTA), sodium ascorbate, copper sulfate, and all other chemicals were purchased from Sigma-Aldrich. HS-$(CH_2)_{11}$-EG_4-OH and HS-$(CH_2)_{11}$-EG_6-N_3 (EG – ethylene glycol) were purchased from Prochimia (Sopot, Poland). Hyaluronic acid (HA) with a weight-averaged molecular weight of 357 kg/mol (Lifecore Biomedical HA500K) was purchased from Lifecore Biomedical (Chaska, MN, USA). 2-Hydroxy-1-[4-(2-hydroxyethoxy)phenyl]-2-methyl-1-propanone (Irgacure 2959) was kindly provided by Ciba Specialty Chemicals (Basel, Switzerland). Deuterium oxide was obtained from SDS (Vitry, France). The water used in all experiments was purified to resistivity of 18.2 MΩ cm. Gold-coated QCM-D sensors with a 4.95 MHz resonance frequency (QSX301) were purchased from Biolin Scientific (Västra Frölunda, Sweden).

2. Methods

Electrochemistry. Electrochemical experiments were performed with a conventional three-electrode potentiostatic system (Model 620E; CH Instruments, Austin, TX, USA). Electrode potentials were measured with reference to Ag/AgCl/KCl (3 M). The counter electrode was platinum, and the working electrode was the gold coating of a QCM-D sensor crystal. The electrochemical cell was purpose designed in our lab. It was adapted from a Q-Sense Open

Module (Biolin Scientific), with the QCM-D sensor crystal being located at the base of the cell covered with the electrolyte solution (0.1 M $NaClO_4$, typical volume - 3 mL) in which the counter and reference electrodes were immersed. The surface density of ferrocene (Fc) molecules was calculated from an anodic peak using Faraday's equation:

$$\Gamma_{Fc} = \frac{Q}{F \times z \times A} \quad [S1]$$

where Q is the electric charge transferred through the electroactive layer, F is the Faraday constant (96485 C/mol), z is the number of electrons transferred per molecule ($z_{Fc/Fc+} = 1$) and A is the surface area of the electrode ($A = 1.01$ cm^2 as previously determined[1]).

Quartz crystal microbalance with dissipation monitoring (QCM-D). QCM-D measurements were performed in flow mode (20 μL/min) in 10 mM HEPES (pH 7.4) with 150 mM NaCl on gold-coated QCM-D sensors. The experiments were performed using the Q-Sense E4 system equipped with four Q-Sense Flow Modules (Biolin Scientific). Overtones j = 3, 5, 7, 9, 11, and 13 were recorded in addition to the fundamental resonance frequency. Changes in dissipation and normalized frequencies, $\Delta f_j/j$, for j = 5 are presented.

Spectroscopic ellipsometry (SE). *In situ* SE measurements were performed in flow mode (20 μL/min) in 10 mM HEPES (pH 7.4) with 150 mM NaCl using the Q-Sense Ellipsometry Module (Biolin Scientific) on gold-coated QCM-D sensors. The flow module was mounted with the Q-Sense E1 system on a spectroscopic rotating compensator ellipsometer (M2000V; Woollam, Lincoln, NE, USA) and ellipsometric data, Δ and ψ, were acquired over a wavelength range of λ = 380 – 1000 nm at 65 degrees angle of incidence. Prior to measurements, the glass windows of the flow chamber were verified not to perturb the polarization of the light beam. To this end, Δ and ψ were recorded for a calibration wafer with a 20 nm silica overlayer (Woollam) first in air and then in air inside the chamber. If required, the position of the windows was adjusted until they induced an offset in Δ below 0.5 degrees.

Bound polymer masses were determined by fitting the ellipsometric data to a multilayer model, using the software CompleteEASE (Woollam). The model relates the measured Δ and ψ as a function of λ to the optical properties of the sensor surface, the adsorbed film, and the surrounding solution. The opaque gold film covering the QCM-D sensor functionalized with SAM-Fc was treated as a single homogeneous layer. Its effective optical properties were determined from data acquired in the presence of bulk solution but in the absence of a polymer film, by fitting the refractive index $n(\lambda)$ and the extinction coefficient $k(\lambda)$ over the accessible wavelength range using a B-spline algorithm implemented in CompleteEASE. The semi-infinite bulk solution was treated as a transparent Cauchy medium, with a refractive index $n_{sol}(\lambda) = A_{sol} + B_{sol}/\lambda^2$. For the surrounding buffer solution, A_{sol} =1.325 and B_{sol} =0.00322 μm^2 were used.[2] The solvated polymer layer was treated as a single layer, which we assumed to be transparent and homogeneous (Cauchy medium), with a given thickness (d_{pol}), a wavelength-dependent refractive index ($n_{pol}(\lambda) = A_{pol} + B_{pol}/\lambda^2$), and a negligible extinction coefficient ($k_{pol} = 0$). d_{pol} and A_{pol} were treated as fitting parameters, assuming $B_{pol} = B_{sol}$. The χ^2 value for the best fit was typically below 2, indicating a good fit.

3. Synthesis of HA-β-CD

β-CD-thiol (**1**, in Fig. S1A) was synthesized using an acid-amine coupling between β-CD-NH_2 and MPA as described previously.[3] Briefly, to a solution of β-CD-NH_2 (100 mg, 8.54×10^{-5}

mol, 1 molar equivalent) in dry DMF, DIEA (14.6 µL, 8.54×10^{-5} mol, 1 molar equivalent), HOBt (23 mg, 1.71×10^{-4} mol, 2 molar equivalents), DIC (52.9 µL, 3.42×10^{-4} mol, 4 molar equivalents) and MPA (9.7 µL, 1.11×10^{-4} mol, 1.3 molar equivalents) were successively added. The resulting mixture was stirred under nitrogen atmosphere at room temperature overnight. After evaporating most of the solvent, the residual syrup was poured into acetone. The white precipitate was collected by filtration, washed with acetone and dried to give pure β-CD-thiol (90 mg, 86% yield). The chemical shifts δ (in ppm) for ^{1}H NMR (D_2O) corresponding to the characteristic signal intensities are 5.10-4.95 (m, 7H, anomeric protons of β-CD), 4.10-3.45 (m, 40H, other protons of β-CD), 3.37 and 3.14 (2H, H6 of the modified glucose unit of β-CD), 2.69 and 2.55 (4H, C**H**$_2$-C**H**$_2$-SH). *m/z* found in MS-MALDI-TOF was 1244.40, while $[M+Na]^+$ calculated for $C_{45}H_{75}O_{35}NSH$ is 1244.37.

HA-pentenoate (**2**, Fig. S1A) was prepared by esterification of the HA hydroxyl groups using 4-pentenoic anhydride as described previously.[3] Briefly, HA (400 mg, 9.98×10^{-4} mol disaccharides) was dissolved in water, and the resulting mixture (2% w/v solution) was kept at 4 °C under continuous stirring overnight. DMF was then added dropwise until a water/DMF ratio of 3:2 (v:v) was obtained. Then 4-pentenoic anhydride (164 µL, 8.98×10^{-4} mol) was added while maintaining the pH between 8 and 9 for 4 h. To obtain a degree of substitution (DS; i.e. the ratio of pentenoate per HA disaccharide repeat unit) of approximately 0.2, the addition of 4-pentenoic anhydride was stopped at 0.9 molar equivalents with respect to repeating units of HA. The reaction mixture was kept at 4 °C under continuous stirring overnight. The product was purified by diafiltration (ultramembrane Amicon YM30) and recovered by freeze-drying (405 mg, 97% yield).

HA-β-CD (**3**, Fig. S1A) was synthesized using photochemically induced thiol-ene coupling between β-CD-thiol and HA-pentenoate as described previously.[3] HA-pentenoate (20 mg, 4.78×10^{-5} mol disaccharides) was first dissolved in water, and the resulting mixture was kept at 4 °C under continuous stirring overnight. Then, Irgacure 2959 (a water soluble photoinitiator, 0.01 % w/v) and β-CD-thiol (5.3 mg, 4.30×10^{-6} mol, 0.09 molar equivalents with respect to the repeating disaccharide unit of HA) were added during stirring. The concentrations of HA and Irgacure 2959 in the resulting solution were 3 mg/mL and 1 mg/mL, respectively. The reaction mixture was exposed to UV light (λ = 365 nm) at room temperature for 5 min. The product was purified by diafiltration (ultramembrane Amicon YM30) with ultrapure water. The purified product was recovered by freeze-drying and characterized by ^{1}H NMR spectroscopy (20.9 mg, 96% yield). The degree of substitution (DS; i.e. the ratio of β-CD per HA disaccharide repeat unit) was determined to be 0.03 (Fig. S1B).

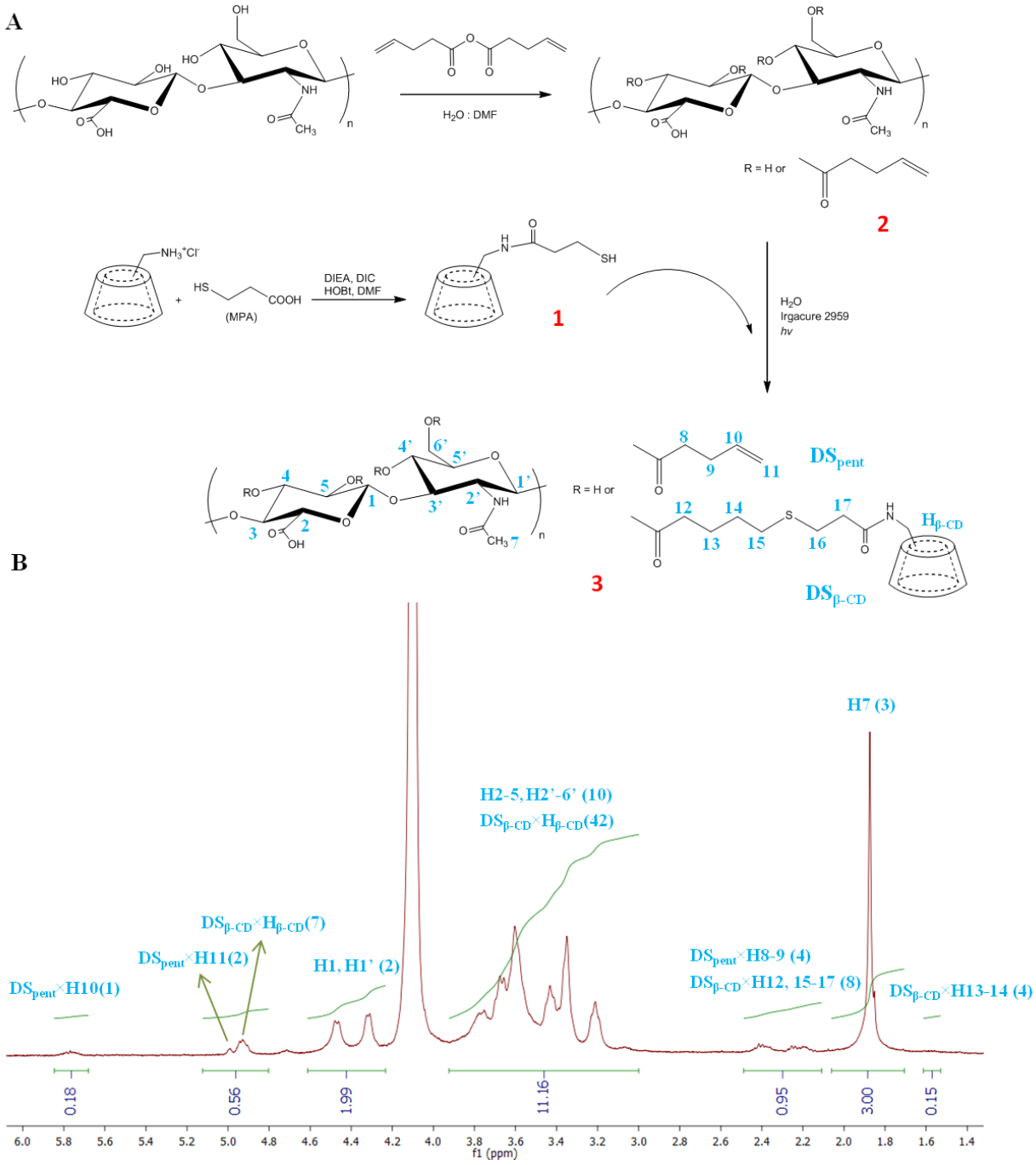

Fig. S1. Synthesis of HA-β-CD. (A) Synthetic routes to β-CD-thiol, HA-pentenoate and HA-β-CD. (B) ^{1}H NMR spectrum (400 MHz, 6 mg/mL in D_2O, 80 °C) of HA-β-CD. $DS_{\beta\text{-CD}}$ = 3±0.5% is determined by digital integration of the signals at 1.9, 5.8 and 5.0 ppm, which gives $DS_{\beta\text{-CD}}$ = (0.56-(0.18×2))/7×100% = 3%.

4. SAM-Fc formation

The functionalization of gold surfaces with mixed self-assembled monolayers (SAMs) is described in detail elsewhere.[1] The gold-coated QCM-D sensors were cleaned by UV-ozone treatment for 5 min followed by the immersion in ethanol for 20 min with stirring. The clean surfaces were then placed in ethanol containing HS-$(CH_2)_{11}$-EG_4-OH and HS-$(CH_2)_{11}$-EG_6-N_3 (1 mM total concentration). After overnight adsorption, the SAM-coated surfaces were rinsed with ethanol and dried under nitrogen. To functionalize SAM-coated surfaces with Fc, they were immersed in a water/t-butanol (1:2) solution containing 0.25 mM ethynylferrocene, 0.1 mM $CuSO_4$, 0.1 mM TBTA (for stabilizing the Cu(I) catalyst) and 0.5 mM sodium ascorbate (for generation of the Cu(I) catalyst) for 1 h. After the reaction, monolayers were thoroughly rinsed with water/t-butanol (1:2) solution and water to ensure that all physisorbed molecules were washed off.

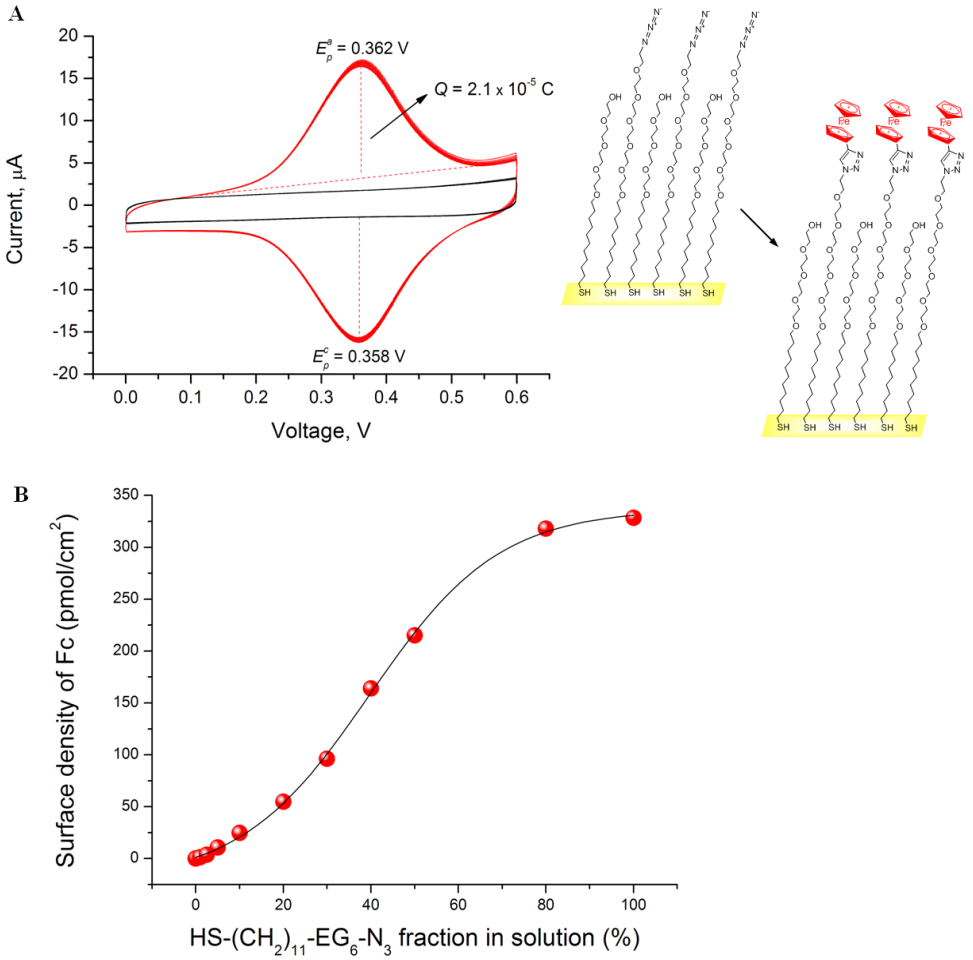

Fig. S2. Electrochemical characterization of SAM-Fc. (A) Representative voltammetric response of the gold electrode coated with a mixed SAM (prepared using 50 mol-% HS-$(CH_2)_{11}$-EG_6-N_3 in the solution; black) and after its modification with Fc (red). Electrolyte – 0.1 M $NaClO_4$, scan rate – 0.1 V/s. (B) Dependence of ferrocene surface density on HS-$(CH_2)_{11}$-EG_6-N_3 molar fraction in solution used to prepare mixed SAMs. The solid black line is a guide for the eyes.

Electrochemical characterization of SAM-Fc. Fig. S2A shows examples of cyclic voltammograms recorded for the gold electrode modified with a mixed SAM (prepared using 50 mol-% HS-$(CH_2)_{11}$-EG_6-N_3) and with an identically prepared SAM after click modification with Fc. One can see that SAM and SAM-Fc are stable during repetitive cycling (10 voltammograms are displayed in each case). Fc oxidation and Fc^+ reduction peaks are symmetric, which is indicative of surface immobilization of the redox probe. The surface density of Fc molecules, determined from the anodic charge associated with the conversion of Fc to Fc^+, is equal to 215.5 pmol/cm^2 (equation S1). The dependence of the Fc surface density on HS-$(CH_2)_{11}$-EG_6-N_3 molar fraction in solution is shown in Fig. S2B. Based on repeated measurements for a selected thiol mixture (10 mol-% HS-$(CH_2)_{11}$-EG_6-N_3), we estimate the standard error in the reproducibility of preparing a desired Fc surface density to be 6%. The error bars provided in Fig. 3B correspond to the standard error in the reproducibility combined with the sensitivity of voltammetric measurements (0.5 pmol/cm^2).

5. Characterization of HA-β-CD binding to SAM-Fc

We used SE to monitor the surface density of HA-β-CD during polymer adsorption (3 h) and buffer rinsing (2 h). Fig. S3 shows HA-β-CD binding kinetics recorded for ferrocene surface densities varied from 15.6 to 328.5 pmol/cm^2.

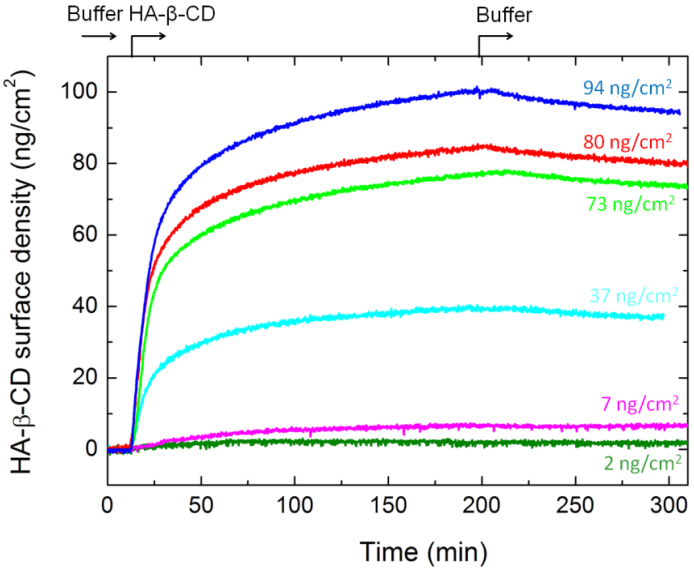

Fig. S3. HA-β-CD binding to SAM-Fc with different ferrocene surface densities (15.6 pmol/cm^2 – olive, 24.7 pmol/cm^2 – magenta, 54.8 pmol/cm^2 – cyan, 96.2 pmol/cm^2 – green, 163.4 pmol/cm^2 – red, 328.5 pmol/cm^2 – blue) monitored by SE. The surface densities of HA-β-CD, $\Gamma_{\text{HA-β-CD}}$, after polymer adsorption and buffer rinsing are shown. Conditions: buffer – 10 mM HEPES (pH 7.4) with 150 mM NaCl, T = 23 °C, concentration of HA-β-CD in the bulk solution – $c_{\text{HA-β-CD}}$ = 50 μg/mL, flow rate - 20 μL/min. The adsorbed polymer mass per unit area was determined using de Fejter's equation: $\Gamma_{\text{pol}} = d_{\text{pol}} \times \frac{A_{\text{pol}} - A_{\text{sol}}}{\mathrm{d}n/\mathrm{d}c}$.[4,5] To calculate Γ_{pol}, we used the refractive index increment of dn/dc = 0.15 cm^3/g reported for HA,[6-8] assuming that the grafted pentenoate and β-CD do not significantly affect the optical properties of the polymer. See section 2 for the details of SE measurements and A_{pol} and d_{pol} determination (A_{sol} =1.325).[2] Numbers in the figure indicate HA-β-CD surface densities at the end of the measurement.

6. Analytical model of multivalent binding

Lattice model. We consider a Langmuir-like lattice model where polymers in solution can adsorb to specific cells located on a surface. We assume that each cell can be occupied by an integer number of polymers and adsorption to different cells is independent. We set the size of a lattice cell (a) equal to the size of a polymer chain, i.e. $a^3 = 4/3\,\pi R_g^3$ with R_g being the radius of gyration. Takahashi et al. determined R_g = 45 nm for 357 kDa HA in 200 mM NaCl.[9] We do not know the exact value of R_g in our experiments, because we worked at slightly lower ionic strength and because the modification of HA with β-CD may also affect R_g. We expect these effects to be minor and therefore set R_g = 45 nm.

Each polymer carries n_R receptors and each adsorbing cell has n_L ligands. We further assume that each polymer has access to only a single lattice cell at a time and within the lattice cell the conformational space of the polymer is adequately large such that each of the n_L ligands is within reach of all the n_R receptors. Ligand-receptor binding is valence limited, i.e. each ligand can bind to at most a single receptor and vice versa. The model presented here is very similar to a model previously developed for multivalent particle adsorption.[10] The difference is that we allow multiple polymers to occupy a single lattice cell, while the particle model allows for at most a single particle per cell. We remark that the denomination of ligands and receptors chosen here is distinct from the previous theoretical work.[10] This change was necessary to match the terminology adopted in chemistry, where the host moiety (i.e. the polymer-bound β-CD in our case) is typically considered the receptor and the guest moiety (i.e. the surface-bound Fc in our case) is considered the ligand.

We focus on the dependence of polymer adsorption on surface ligand density. Therefore we write a grand-canonical partition function $\Xi(n_L)$ for a single surface lattice cell as

$$\Xi(n_L) = 1 + \sum_{i=1}^{\infty} z^i q_i \qquad [S2]$$

where i is the number of polymers that are adsorbed in the cell, z is the activity of the polymers in solution and q_i is the single cell bound state partition function with i polymers occupying the cell. The activity is defined as $z \equiv v_0 \rho_0 N_A \exp \beta\mu$, where v_0 is the volume that each polymer is allowed to explore while bound to a lattice cell ($v_0 \approx a^3$) and $\rho_0 = 1\,\mathrm{mol/l}$ is the standard concentration. μ is the chemical potential of the polymers in solution and $\beta = 1/k_B T$ the inverse thermal energy, where k_B is the Boltzmann constant and T the absolute temperature. For dilute solutions we can approximate z through the ideal gas contribution to the chemical potential and the activity is then given by $z \approx \rho N_A a^3$, where N_A is Avogadro's number and ρ is the polymer concentration (in $\mathrm{mol/l}$).

Binding of one polymer. The bound state partition function q_i counts all possible combinations of ligand-receptor bonds. In general a polymer is considered to be bound if it forms at least one bond with the surface ligands. For a single bound polymer, the partition function reads

$$q_1 = \sum_{m=1}^{m_{\max}} e^{-m\beta F} \binom{n_L}{m} \binom{n_R}{m} m! = \sum_{m=1}^{m_{\max}} q_1(m) = \sum_{m=1}^{m_{\max}} e^{-m\beta F} \frac{n_R! n_L!}{(n_R - m)! m! (n_L - m)!} \qquad [S3]$$

where m is the number of formed bonds and βF is the free energy gain (relative to the thermal energy) for forming a single bond. The combinatorial factor counts all possible distinct ways of binding together n_L ligands with n_R receptors using m bonds. The maximum number of bonds

$m_{\max} = \min(n_L, n_R)$ is limited by either the number of ligands or receptors, whichever is lower. $q_1(m)$ is the partition function restricted to the case in which the polymer forms m bonds.

The binding free energy F determines the probability for a given receptor (attached to a polymer) to bind to a ligand (on the surface). It will depend on the dissociation constant K_d of individual ligand-receptor interactions, and on the volume accessible to the receptor. We assume that the polymer is adequately flexible so that unbound receptors are able to explore the same volume as the polymer to which they are attached, i.e. a^3, and obtain

$$F = \ln(K_d\, a^3\, N_A)\, k_B T + U_{poly} \quad [S4]$$

In the context of our simple model, we consider U_{poly} an empirical term that represents added entropic effects of subsequent ligand binding, once the nanoobject is present at the surface. U_{poly} depends on the details of the polymer system, such as the receptor-polymer linker length, the distribution of receptors along the polymer chain, or excluded volume interactions (between polymer segments, and between the polymer and the surface). As a first and presumably crude approximation, we assume that U_{poly} does not depend on the number of bonds m, i.e. according to Eqs. S3 and S4, for m bonds, the added entropic effects would scale with mU_{poly}. We do not know the exact value of U_{poly} in our experimental system, and therefore treat it as a fitting parameter. We expect U_{poly} to be on the order of a few $k_B T$, typical for the entropic costs of supramolecular binding.[11]

Binding of two polymers. When two polymers occupy the same lattice cell, the first can bind to any of the n_L surface ligands but the second polymer has less ligands available to it. We write the two polymer bound state partition function as

$$q_2 = \frac{1}{2}\sum_{m_1=1}^{m_{\max}} \left[e^{-m_1\beta F} \frac{n_R!\, n_L!}{(n_R-m_1)!\, m_1!\, (n_L-m_1)!} \sum_{m_2=1}^{m'_{\max}} e^{-m_2\beta F} \frac{n_R!\,(n_L-m_1)!}{(n_R-m_2)!\, m_2!\, (n_L-m_1-m_2)!} \right] e^{-\beta U_2} \quad [S5]$$

where m_1 and m_2 count the number of bonds formed with the first and second polymer respectively and $m'_{\max} = \min(n_R, n_L - m_1)$ is the maximum number of bonds available to the second polymer. The two polymer overlap term βU_2 takes into account the free energy penalty due to polymer excluded volume. The factor $1/2$ in front is needed because polymers are indistinguishable and exchanging the two polymers produces the same microstate. We notice that with two polymers we have effectively $2n_R$ receptors on a lattice cell so the partition function can be rewritten as

$$q_2 = \frac{1}{2} e^{-\beta U_2} \left[\sum_{m=1}^{\min(2n_R, n_L)} e^{-m\beta F} \frac{(2n_R)!\, n_L!}{(2n_R-m)!\, m!\, (n_L-m)!} - 2\sum_{m=1}^{\min(n_R, n_L)} e^{-m\beta F} \frac{n_R!\, n_L!}{(n_R-m)!\, m!\, (n_L-m)!} \right] \quad [S6]$$

where the right hand sum has to be subtracted because each of the polymers has to have at least one bond present. The equality of Eqs. S5 and S6 can be proven by applying the Chu-Vandermonte identity. Inserting Eq. S3 into S5, we find

$$q_2 = \frac{1}{2} e^{-\beta U_2} \left[\sum_{m=1}^{\min(2n_R, n_L)} e^{-m\beta F} \frac{(2n_R)!\, n_L!}{(2n_R-m)!\, m!\, (n_L-m)!} - 2q_1 \right] \quad [S7]$$

For the range of parameters studied, the number of surface ligands per cell n_L will always be much larger than the number of available receptors in_R. In the limit $n_L \gg in_R$, Eq. S3 can be simplified to

$$q_1 = \sum_{m=1}^{n_R} (n_L e^{-\beta F})^m \frac{(n_R)!}{(n_R-m)!\, m!} = \left[(1 + n_L e^{-\beta F})^{n_R} - 1 \right] \quad [S8]$$

and Eq. S7 to

$$q_2 = \frac{1}{2}e^{-\beta U_2}\left[(1 + n_{\mathrm{L}}e^{-\beta F})^{2n_{\mathrm{R}}} - 1 - 2q_1\right] = \frac{1}{2}e^{-\beta U_2}\left[(1 + n_{\mathrm{L}}e^{-\beta F})^{n_{\mathrm{R}}} - 1\right]^2 \qquad \text{[S9]}$$

This simplification also provides a practical route to calculating various q_{i} because it would be difficult to calculate factorials for $n_{\mathrm{L}} > 170$ in Eqs. S3 and S7.

Binding of i polymers. The above procedure can be further extended to any number of polymers adsorbed in a given cell. We find that the expression for a bound state partition function with i polymers adsorbed on a cell is then

$$q_i = \frac{1}{i!}\left[(1 + n_{\mathrm{L}}e^{-\beta F})^{n_{\mathrm{R}}} - 1\right]^i e^{-\beta U_i} \qquad \text{[S10]}$$

where the $1/i!$ factor accounts for possible permutations of the i polymers.

The term U_{i} specifies the overlap free energy penalty for having i polymers adsorbed to a single cell. Computing this term accurately is complicated as it depends on the conformational space of many overlapping polymers. Therefore, we will use an approximate scaling expression. We assume the polymers, each made of N segments of size b, to be immersed in a good solvent, i.e. $R_{\mathrm{g}} \approx bN^{3/5}$. The approximate signs in this and the following equations indicate that the scaling expressions are accurate to within a numerical prefactor of order unity. The law of des Cloiseaux gives the osmotic pressure $\beta P \approx b^{-3}\phi^{9/4}$, where ϕ is the polymer packing fraction.[12] If we confine i polymers in a volume V, we have $\phi_i \approx iNb^3/V$. The free energy penalty for packing i polymers into a lattice cell of size $a^3 \approx R_{\mathrm{g}}^3$ is then

$$U_i = \int_{a^3}^{\infty} P\mathrm{d}V = A_{\mathrm{dG}}i^{9/4} \qquad \text{[S11]}$$

where we have introduced the scaling factor A_{dG} which is expected to be of order $1k_{\mathrm{B}}T$.

The scaling relation assumes that the polymer is free to explore the volume within a cell and that the monomer density within a cell is constant. If the surface density of binding sites is sufficiently high, then multiple polymers will overlap in the same cell and there are typically also many ligand-receptor bonds per polymer formed. Under this condition, the monomer density profile is likely to be peaked close to the surface. Therefore we expect that Eq. S11 underestimates the effective packing fraction and consequently the overlap penalty U_i for large i.

Moreover, the extension $R_{\parallel}$ of an adsorbed polymer along the surface might differ from the size R_{g} of the unperturbed polymer in solution, and one may ask if the choice of a fixed lattice size a in our theory is justified. On the one hand, attraction of the polymer by the surface tends to increase $R_{\parallel}$. On the other hand, excluded volume repulsions between neighbouring polymer chains tend to decrease $R_{\parallel}$. For the adsorption of a homogeneous polymer to a homogeneously attractive surface, this problem was explicitly addressed by Bouchaud and Daoud.[13] Based on their scaling approach, one can estimate that the deviation of $R_{\parallel}$ from R_{g} is typically moderate, i.e. below a factor of two. We will show later (c.f. Fig. S5A) that a twofold variation in a has only a minor influence on polymer adsorption. Therefore, the use of a fixed a in our theory is a reasonable approximation.

Polymer surface coverage. We now have the necessary tools to calculate the grand partition function for a single lattice cell (Eq. S2) from which the average number of bound polymers $\theta(n_{\mathrm{L}})$ per cell can be easily calculated as

$$\theta(n_L) = \frac{\partial \ln \Xi(n_L)}{\partial(\beta\mu)} = \frac{\sum_{i=1}^{\infty} i z^i q_i}{1+\sum_{i=1}^{\infty} z^i q_i} \quad [S12]$$

However, we note that a surface is a collection of lattice cells and in general not all cells are equal. It is reasonable to assume that the distribution of ligands on a surface is uniformly random, i.e. the number of ligands per lattice cell follows a Poisson distribution

$$p(n_L, \langle n_L \rangle) = \frac{\langle n_L \rangle^{n_L}}{n_L!} e^{-\langle n_L \rangle} \quad [S13]$$

with $\langle n_L \rangle$ the average number of surface ligands per cell. If the surface is composed of N independent lattice cells, the grand partition function for the whole surface reads

$$\Xi(\langle n_L \rangle) = \prod_{n_L=1}^{\infty} \Xi(n_L)^{p(n_L, \langle n_L \rangle)N} \quad [S14]$$

and the average surface coverage is then given by

$$\langle \theta \rangle = \sum_{n_L=1}^{\infty} p(n_L, \langle n_L \rangle)\theta(n_L) \quad [S15]$$

We stress that for the range of parameters studied the number of surface ligands per cell was always large ($\langle n_L \rangle$ > 100) and the Poisson distribution (Eq. S13) is highly peaked around $n_L = \langle n_L \rangle$. Therefore, the relative fluctuations in the ligand density are small and we have approximately $\langle \theta \rangle \approx \theta(\langle n_L \rangle)$. We note that, for simplicity, we have dropped the brackets around $\langle n_L \rangle$ in the main text of the paper.

Implementation of the model. We first calculated the single cell bound state partition functions q_i (Eq. S10), from which we obtained the average number of bound polymers per cell $\theta(n_L)$ for a given number of surface ligands n_L (Eq. S12). We then made use of the Poisson distribution (Eq. S13) to calculate the average surface coverage in the system $\langle \theta \rangle$ (Eq. S15). In order to fit the experimental data (Fig. 3), only A_{dG} and U_{poly} (Eq. S4) were fitted. All other parameters were kept fixed to the values indicated in the main text of the paper. To illustrate, how strongly polymer binding depends on A_{dG} and U_{poly}, we show predicted curves of $\Gamma_{HA-\beta-CD} = \theta M_{HA-\beta-CD}/(N_A a^2)$ *vs.* $\Gamma_{Fc} = n_L/(N_A a^2)$ for selected values in Fig. S4.

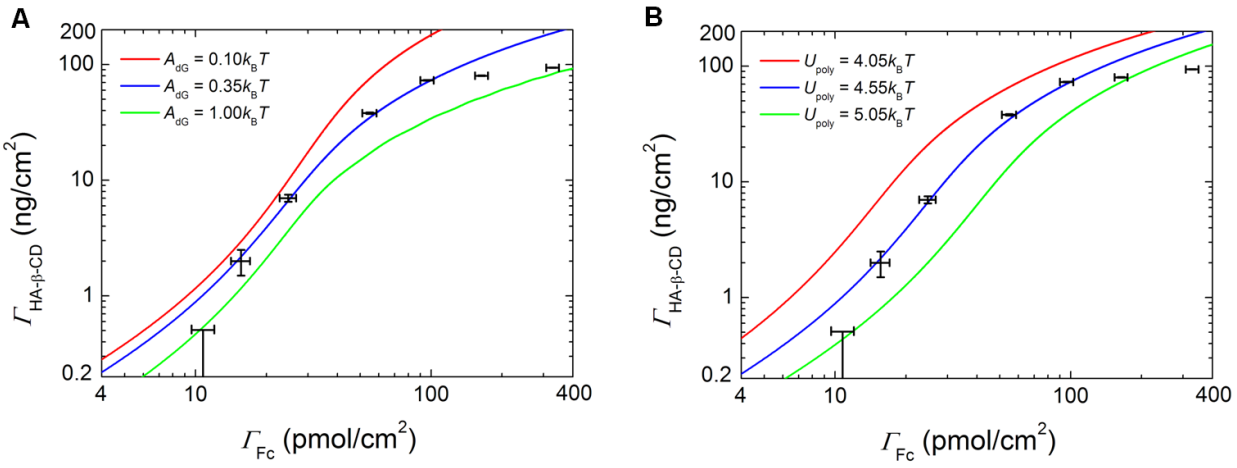

Fig. S4. Dependence of $\Gamma_{HA-\beta-CD}$ *vs.* Γ_{Fc} on A_{dG} (A; for $U_{poly} = 4.55k_BT$) and U_{poly} (B; for $A_{dG} = 0.35k_BT$). Experimental data plotted in the form of error bars are shown in black.

Impact of lattice size. Fig. S5A illustrates that variations in the lattice size *a* by a factor of two (i.e. within limits that are reasonable based on simple consideration for the adsorption of polymers) affect the polymer adsorption only weakly (except at high polymer coverage where our model is not expected to reproduce the experimental data quantitatively).

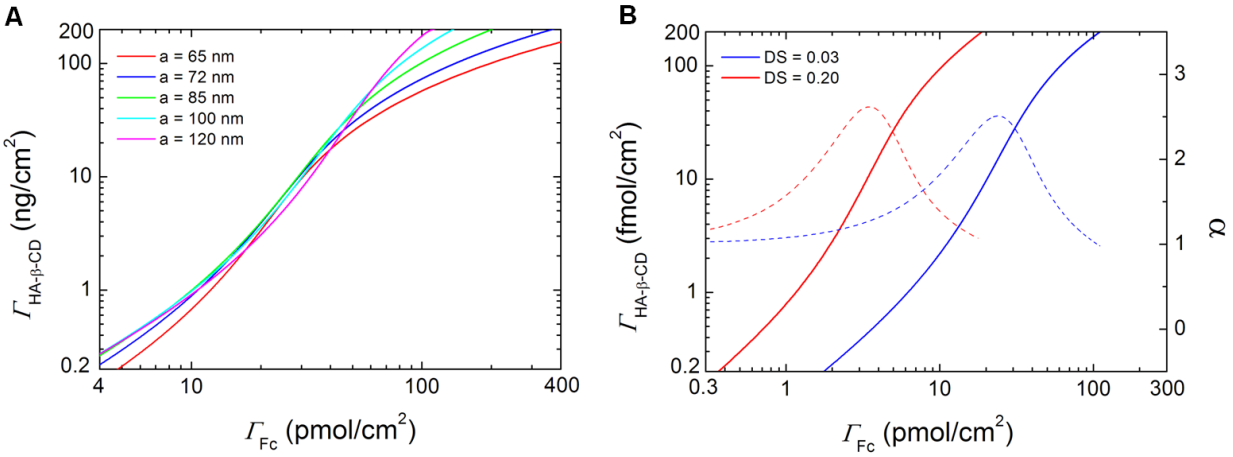

Fig. S5. Dependence of $\Gamma_{\text{HA-β-CD}}$ *vs.* Γ_{Fc} on the lattice size *a* (A; for DS = 0.03) and the degree of substitution DS (B; for *a* = 72 nm) for $U_{\text{poly}} = 4.55k_{\text{B}}T$ and $A_{\text{dG}} = 0.35k_{\text{B}}T$. The dashed lines show the respective dependencies of the selectivity parameter α on Γ_{Fc}.

Comparison with biologically relevant conditions. Fig. S5B compares theoretical predictions for DS = 3%, used in our experiments, and DS = 20%. The latter would correspond to one binding site per HA decasaccharide, a size comparable to the footprint of HA-binding proteins, including the cell surface receptor CD44,[14,15] on HA. The data shows that the quality of superselective binding is retained at higher DS but that superselective binding occurs at lower surface densities of ligands. The targeted densities in this case become comparable to the densities of CD44 on the cell surface,[16-18] illustrating that the findings obtained with our model system can be extended to biologically relevant conditions.

7. Supplementary references

(1) Dubacheva, G. V.; Van Der Heyden, A. l.; Dumy, P.; Kaftan, O.; Auzély-Velty, R.; Coche-Guerente, L.; Labbé, P. *Langmuir* **2010**, *26*, 13976.
(2) Eisele, N. B.; Frey, S.; Piehler, J.; Gorlich, D.; Richter, R. P. *EMBO Rep* **2010**, *11*, 366.
(3) Mergy, J.; Fournier, A.; Hachet, E.; Auzély-Velty, R. *J. Polym. Sci., Part A: Polym. Chem.* **2012**, *50*, 4019.
(4) De Feijter, J. A.; Benjamins, J.; Veer, F. A. *Biopolymers* **1978**, *17*, 1759.
(5) Richter, R. P.; Rodenhausen, K. B.; Eisele, N. B.; Schubert, M. In *Ellipsometry of Functional Organic Surfaces and Films*; Hinrichs, K., Eichhorn, K.-J., Ed.; Springer: 2013, p 223.
(6) Takahashi, R.; Kubota, K.; Kawada, M.; Okamoto, A. *Biopolymers* **1999**, *50*, 87.
(7) Fouissac, E.; Milas, M.; Rinaudo, M.; Borsali, R. *Macromolecules* **1992**, *25*, 5613.
(8) Hayashi, K.; Tsutsumi, K.; Nakajima, F.; Norisuye, T.; Teramoto, A. *Macromolecules* **1995**, *28*, 3824.

(9) Takahashi, R.; Al-Assaf, S.; Williams, P. A.; Kubota, K.; Okamoto, A.; Nishinari, K. *Biomacromolecules* **2003**, *4*, 404.
(10) Martinez-Veracoechea, F. J.; Frenkel, D. *PNAS* **2011**, *108*, 10963.
(11) Martinez-Veracoechea, F. J.; Leunissen, M. E. *Soft Matter* **2013**, *9*, 3213.
(12) de Gennes, P.-G. *Scaling concepts in polymer physics*; Cornell University Press, 1979.
(13) Bouchaud, E.; Daoud, M. *J. Phys. France* **1987**, *48*, 1991.
(14) Tammi, R.; MacCallum, D.; Hascall, V. C.; Pienimäki, J.-P.; Hyttinen, M.; Tammi, M. *J. Biol. Chem.* **1998**, *273*, 28878.
(15) Lesley, J.; Hascall, V. C.; Tammi, M.; Hyman, R. *J. Biol. Chem.* **2000**, *275*, 26967.
(16) Alves, C. S.; Burdick, M. M.; Thomas, S. N.; Pawar, P.; Konstantopoulos, K. *Am. J. Physiol. - Cell Ph.* **2008**, *294*, C907.
(17) Visintin, A.; Mazzoni, A.; Spitzer, J. H.; Wyllie, D. H.; Dower, S. K.; Segal, D. M. *J. Immunology* **2001**, *166*, 249.
(18) Wolny, P. M.; Banerji, S.; Gounou, C.; Brisson, A. R.; Day, A. J.; Jackson, D. G.; Richter, R. P. *J. Biol. Chem.* **2010**, *285*, 30170.